

# Production and Characterization of Nano-TiO<sub>2</sub> Coatings on Aluminium Alloy Surfaces with Improved Anticorrosion Behaviour

Gianluigi De Falco<sup>a\*</sup>, Giuseppe De Filippis<sup>b</sup>, Carmela Scudieri<sup>b</sup>, Luca Vitale<sup>b</sup>, Mario Commodo<sup>c</sup>, Patrizia Minutolo<sup>c</sup>, Andrea D'Anna<sup>a</sup>, Paolo Ciambelli<sup>b</sup>

<sup>a</sup>Dipartimento di Ingegneria Chimica, dei Materiali e della Produzione Industriale - Università degli Studi di Napoli Federico II, P.le Tecchio 80, 80125, Napoli, Italy

<sup>b</sup>Narrando Srl, Via Giovanni Paolo II, 132, 84084 Fisciano (SA), Italy

<sup>c</sup>Istituto di Scienze e Tecnologie per l'Energia e la Mobilità Sostenibili, STEMS-CNR, P.le Tecchio 80, 80125, Napoli, Italy  
[gianluigi.defalco@unina.it](mailto:gianluigi.defalco@unina.it)

This paper presents a one-step method for the coating of aluminium alloy surfaces with titania nanoparticles. This method is based on a highly controllable and tunable technique for the production of thin coating layers of TiO<sub>2</sub> nanoparticles by aerosol flame synthesis and direct thermophoretic deposition. More specifically, few nm diameter TiO<sub>2</sub> nanoparticles in the form of anatase are synthesized by flame aerosol and directly deposited as thin film by thermophoresis on aluminium alloy AA2024 samples. Submicron coatings of different thicknesses were produced by changing the total deposition time. A thermal annealing treatment was fine-tuned using UV-Vis Absorption spectroscopy and applied in order to improve the adhesion of the coating on the aluminium surface.

Electrochemical polarization measurements were performed to evaluate the corrosion resistance of coated aluminium substrates. The electrochemical polarization curves showed a significant increase of the corrosion potential of coated substrates with respect to the bare aluminium and a decrease in the current density. The coatings produced with higher deposition time and so greater thickness showed the best performances in terms of corrosion resistance.

## 1. Introduction

The use of aluminium alloys in the aeronautic and aerospace industries for the production of structural components is widely adopted (Starke and Staley, 1996; Williams and Starke, 2003). Indeed, aluminium alloys are characterized by attractive properties such as high damage tolerance and tensile strength, low weight and ease of fabrication. On the other hand, the production of nano-coatings to improve the electrochemical properties of aluminium surfaces has become a topic of great interest, due to the low resistance to corrosion that aluminium substrates showed (Abdeen et al., 2019). Among several nanomaterials suitable for nanocoatings, titanium dioxide is one of the most attractive, due to its high photocatalytic activity, excellent anticorrosion properties, chemical stability and heat resistance (Liberini et al., 2015; De Falco et al., 2017), coupled with a low environmental and biological toxicity (McCracken et al., 2016). However, the deposition of TiO<sub>2</sub> nanoparticles on aluminium surfaces is quite challenging. Aerosol Flame Synthesis (AFS) furnishes an easy, cost-effective and scalable method to synthesize nano-TiO<sub>2</sub> with required properties and to deposit particles in one-step as nanostructured coatings on metal alloys surfaces (Li et al., 2016).

This paper reports a procedure based on aerosol flame synthesis and direct thermophoretic deposition for the production of nano-TiO<sub>2</sub> coating layers on aluminum AA2024 substrates and the characterization of their improved electrochemical behavior by electrochemical polarization measurements.

## 2. Experimental

The experimental set-up for the production of TiO<sub>2</sub> nanocoatings is composed by an AFS apparatus and a thermophoretic deposition system. More specifically, the AFS apparatus consists of a custom-made honeycomb burner and a high-pressure syringe pump to feed the precursor solution, while the thermophoretic deposition system is based on a rotating disk technology. Figure 1 shows a schematic of the experimental set-up. More details about the experimental apparatus can be found in previous works (De Falco et al., 2017; De Falco et al., 2018; De Falco et al., 2019).

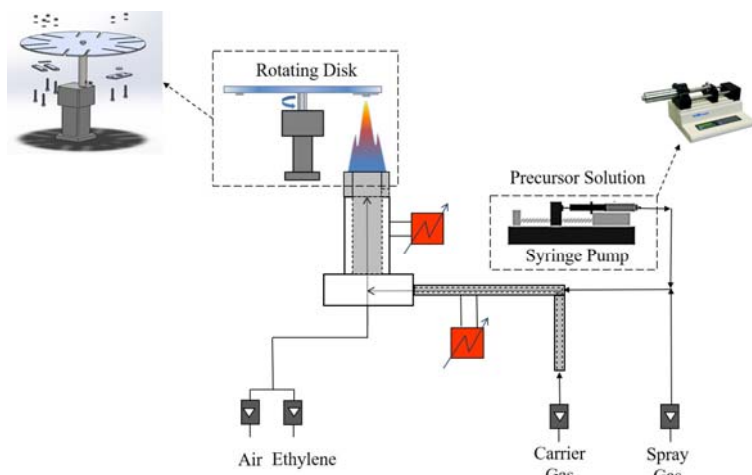


Figure 1: Schematic of the experimental set-up.

The rotating disk section of the experimental set-up was designed to allocate six circular aluminium AA2024 substrates (diameter = 1.6 cm, thickness = 3 mm). In the current study, the disk was properly modified in order to further allocate a single annulus-shaped substrate made of aluminium AA2024 (outer diameter OD=25.6 cm, inner diameter ID=22.4 cm, thickness = 6 mm) with a total coating area of 121 cm<sup>2</sup>. UV-vis absorption spectra were acquired on nanoparticle coatings deposited on quartz substrates, by means of an Agilent UV-visible 8453 spectrophotometer. The annealing procedure was performed using a Stuart undergrad stirrer hotplate model US152. The corrosion resistance of uncoated and TiO<sub>2</sub>-coated circular aluminium AA2024 substrates was carried out by performing electrochemical measurements with the aim of a PGSTAT302N Autolab (Metrohm) Potentiostat/Galvanostat controlled by Nova 2.0 software (Metrohn Autolab). In particular, an electrochemical cell with three standard electrodes (Metrohn Autolab) was used, adopting the following configuration: a calomel electrode, used as a reference electrode (RE), a platinum electrode that acts as a counter electrode (CE) and each sample (with an area of ~ 2 cm<sup>2</sup>) was connected to a clamp acting as a working electrode (WE).



Figure 2: Electrochemical cells used for corrosion tests.

Measurements were carried out at room temperature in an electrolytic solution of sodium chloride (NaCl), quiescent and aerated (representative of the corrosive environment), and almost neutral ( $\text{pH}=6.5 \pm 0.2$ ) at 0.6 M NaCl. All electrochemical tests were performed after 1 hour of immersion of the samples at open circuit potential,  $E_{\text{ocp}}$ . Furthermore, the linear anodic polarization tests were conducted at wide ranges of the potentials and at a scan rate of  $1 \text{ mVs}^{-1}$ . To evaluate the effect of the deposition time of  $\text{TiO}_2$  on the aluminum surface in terms of corrosion resistance, the treatment was carried out at different total deposition time  $t_d$ . Using the Tafel polarization tests, the values of corrosion potential ( $E_{\text{corr}}$ ), corrosion current density ( $i_{\text{corr}}$ ), corrosion rate and polarization resistance ( $R_p$ ) were determined from the graphs.

### 3. Results and discussion

The flame reactor for the synthesis of nano- $\text{TiO}_2$  consists of a premixed laminar flame of ethylene and air, with a cold gas velocity  $v_{\text{cg}} = 95 \text{ cm/s}$  and a flame equivalent ratio  $\Phi = 0.95$ . The flame is doped with a 0.5 M solution of titanium tetraisopropoxide (TTIP) into ethanol, fed to the reactor at a flow rate of  $900 \mu\text{l/min}$ . The AFS reactor in those operating conditions produces pure anatase  $\text{TiO}_2$  nanoparticles with dimension of 3.2 nm (De Falco et al., 2019).  $\text{TiO}_2$  nanostructured coatings with different thickness were obtained operating the rotating disk with a rotational speed of 600 rpm and changing the total deposition time  $t_d$  from 15 s up to 80 s. After the deposition process, the coated samples underwent an annealing process performed by putting the coated substrate in direct contact with the hot plate surface. The hot plate was placed inside a chemical hood under controlled atmosphere conditions. The hot plate annealing technique reduces the fluctuation of the annealing temperature with respect to an oven, where the heat transfer by convection usually has an error of  $\pm 15 \text{ }^\circ\text{C}$  (Mahdi et al., 2014). The annealing of thin films has been demonstrated to result in an increase of the film crystallization and densification and so in a better adhesion of the coating to the substrate (Martin et al., 1997). The annealing parameters were set at  $300 \text{ }^\circ\text{C}$  and 30 minutes. The parameters were chosen in order to avoid any temperature-induced phase transformation from anatase to rutile, which occurs at around  $650\text{-}700 \text{ }^\circ\text{C}$  (McCormick et al., 2004; Abdurraheem et al., 2013), since anatase is the preferred phase being the most photoactive phase of  $\text{TiO}_2$ . Moreover, previous works found that  $800^\circ\text{C}$  is a critical annealing temperature at which nanoscale structural and optical properties exhibit significant changes (Abdurraheem et al., 2013). Figure 3 reports a comparison between UV-visible absorption spectra acquired on nano- $\text{TiO}_2$  coatings with a deposition time  $t_d=40 \text{ s}$  underwent different annealing conditions: as deposited, annealed at  $300 \text{ }^\circ\text{C}$  for 1 hour and annealed at  $300 \text{ }^\circ\text{C}$  for 2 hours. All spectra show a high absorbance in the UVA/UVB region, as well as an absorption tail in the visible region. No significant changes in the absorption maximum and the shape of the curve within the experimental uncertainties can be detected on the annealed samples. So, we can assume that the annealing process performed at  $300 \text{ }^\circ\text{C}$  for 30 minutes resulted in a better adhesion of the coatings to the substrates without any modification of the optical and structural properties of the nanocoatings.

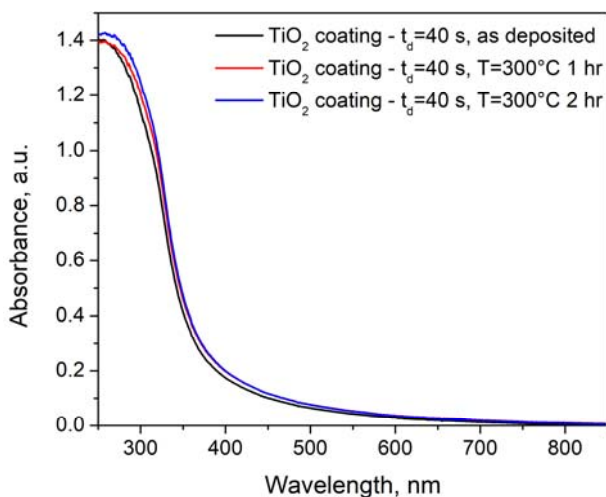


Figure 3: UV-visible absorption spectra acquired on nano- $\text{TiO}_2$  coatings with  $t_d=40 \text{ s}$  as deposited, annealed at  $300 \text{ }^\circ\text{C}$  for 1 hour and annealed at  $300 \text{ }^\circ\text{C}$  for 2 hours.

Various coated substrates were prepared to perform the characterization of the electrochemical performances. Specifically, AA2024 aluminium disks were coated with  $\text{TiO}_2$  nano-coatings at a deposition time  $t_d=40 \text{ s}$  and  $t_d= 80 \text{ s}$ . For both deposition times, different samples were prepared performing the deposition procedure on

just one side and on both sides of the substrates. Typical curves obtained from the corrosion tests through the linear anodic polarization on uncoated bare substrate and on samples coated on both sides with  $t_d=40$  s and  $t_d=80$  s are reported in Figure 4. Usually, the higher is the corrosion potential, the more difficult the metal oxidation reaction will occur, while the higher is the corrosion current density  $i_{corr}$  the higher is the corrosion rate and, therefore, the lower is the corrosion resistance.

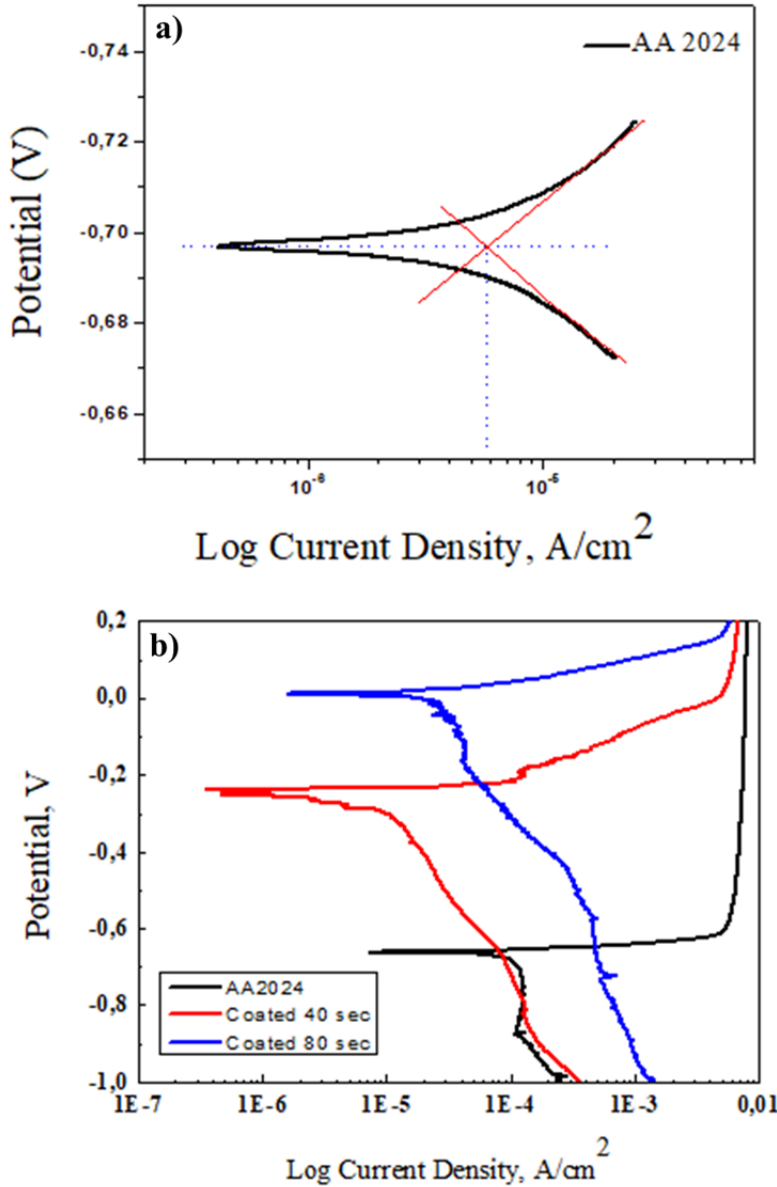


Figure 4: Polarization curves for uncoated (a) and  $TiO_2$ -coated (b) aluminum alloy samples.

The value of the corrosion potential  $E_{corr}$  is in good agreement with the range of values reported in the literature for AA2024 alloy samples, 0.6 - 0.75 V (Atta et al., 2017) and show slight variations related to the variability of the composition and the test conditions (concentration of electrolyte, temperature, pH). The potential values of the coated samples show an increase in the corrosion potential, with respect to the uncoated disks, indicating a greater resistance to corrosion. On the other hand, the current density values show a reduction, indicative of a lower corrosion rate. The effect of titania nano-coatings on corrosion behavior of AA2024 was estimated by defining the protection efficiency PE parameter, that quantifies the decrease in the corrosion rate compared to the bare substrate, according to the following expression:

$$PE = 100 * \frac{(I^0 - I)}{I^0} \quad (1)$$

where  $I^0$  and  $I$  are the current density values obtained from the potentiometric curves for the bare substrate and the coated samples, respectively.

Table 1 summarizes all the polarization tests that have been carried out. For the samples covered on both sides, the results show that as the deposition time increases and therefore as the thickness of nano-TiO<sub>2</sub> on aluminum surface increases, the potential values shift towards nobler potentials. On the other hand, the density of electric current is lower on coated samples with respect to the bare substrate, indicating a good resistance to corrosion and so a lower rate of corrosion. More specifically, the protection efficiency is calculated to be 75-79% for the sample coated on one side with a deposition time  $t_d=40$  s and increases up to 87-89 % for the sample coated on both sides with the same deposition time. The samples coated on both side with an increased deposition time  $t_d=80$  s, and so characterized by a higher thickness of the coating, showed a protection efficiency of 90-91%.

*Table 1: Experimental values of corrosion potential  $E_{corr}$ , current density  $I_{corr}$  and protection efficiency PE for the tested samples*

Sample	$E_{corr}$ (V)	$E_{corr}$ (V) $\pm$ SD	$I_{corr}$ (A/cm <sup>2</sup> )	PE (%)
AA2024	-0.696	-0.67 $\div$ -0.71	$6.10 * 10^{-5} \div 8.40 * 10^{-5}$	0
$t_d=40$ s TiO <sub>2</sub> -coated AA2024 on one side	-0.678	-0.63 $\div$ -0.69	$1.60 * 10^{-5} \div 1.90 * 10^{-5}$	75 $\div$ 79
$t_d=40$ s TiO <sub>2</sub> -coated AA2024 on both sides	-0.275	-0.25 $\div$ -0.40	$8.20 * 10^{-6} \div 9.91 * 10^{-6}$	87 $\div$ 89
$t_d=80$ s TiO <sub>2</sub> -coated AA2024 on both sides	0.014	0.10 $\div$ -0.30	$6.62 * 10^{-6} \div 8.01 * 10^{-6}$	90 $\div$ 91

#### 4. Conclusions

A one-step method for the coating of aluminium alloy surfaces with thin coating layers of TiO<sub>2</sub> nanoparticles by aerosol flame synthesis and direct thermophoretic deposition was presented. A rotating disk apparatus designed to perform the thermophoretic deposition of the coatings was improved allowing to allocate and to coat circular aluminium AA2024 substrates of 1.6 cm in diameter as well as a annulus-shaped AA2024 substrate made of aluminium AA2024 with a total coating area of 121 cm<sup>2</sup>.

After the deposition procedure, the coated samples underwent an annealing process that resulted in an increase of the film crystallization and densification and so in a better adhesion of the coating to the substrate, without any modification of the optical and structural properties of the nanocoatings as proved by UV-vis absorption measurements.

The anticorrosive behaviour of TiO<sub>2</sub> nanocoatings was characterized by means of linear anodic polarization tests. The results showed that the presence of titania coatings results in an effective increase of corrosion resistance of AA2024 substrates. The protection to corrosion is higher for the coatings obtained with the higher deposition time and so the greater coating thickness. The best results are obtained for AA2024 substrates coated on both sides with a deposition time  $t_d=80$  s, which are characterized by a corrosion protection efficiency greater than 90%.

Future works will be devoted to gain a deeper understanding of the corrosion protection mechanism of nano-TiO<sub>2</sub> coatings.

#### Acknowledgments

This work was financially supported by "POR CAMPANIA FERS 2014/2020 nell'ambito dell'Avviso pubblico per il sostegno alle imprese campane nella realizzazione di progetti di trasferimento tecnologico coerenti con la RIS3", funded by Regione Campania.

#### References

- Abdeen D.H., El Hachach M., Koc M., Atieh M.A. 2019, A Review on the Corrosion Behaviour of Nanocoatings on Metallic Substrates, *Materials*, 12, 210.
- Abdulraheem, Y.M., Ghoraishi, S., Arockia-Thai, L., Zachariah, S.K., Ghannam, M. 2013, The effect of annealing on the structural and optical properties of titanium dioxide films deposited by electron beam assisted PVD Yaser, *Advances in Materials Science and Engineering*, 2013, 574738.
- Atta N.F., Abd El Fatah M.A., Galal A. 2017, Effect of titania nanoparticles loading in sol-gel films for corrosion protection of aluminum AA2024-T3 alloy in 3.5% sodium chloride solution, *International Journal of Electrochemical Science*, 12, 1625-1641.

- De Falco G., Porta A., Petrone A., Del Gaudio P., El Hassanin A., Commodo M., Minutolo P., Squillace A., D'Anna A. 2017, Antimicrobial activity of flame-synthesized nano-TiO<sub>2</sub> coatings, *Environmental Science: Nano*, 4, 1095–1107.
- De Falco G., Ciardiello R., Commodo M., Del Gaudio P., Minutolo P., Porta A., D'Anna A. 2018, TiO<sub>2</sub> nanoparticle coatings with advanced antibacterial and hydrophilic properties prepared by flame aerosol synthesis and thermophoretic deposition, *Surface and Coatings Technology*, 349, 830-837.
- De Falco G., Commodo M., Minutolo P., D'Anna A. 2019, Flame aerosol synthesis and thermophoretic deposition of superhydrophilic TiO<sub>2</sub> nanoparticle coatings, *Chemical Engineering Transactions*, 73, 37-42.
- Li, S., Ren, Y., Biswas, P., Tse, S. D. 2016, Flame aerosol synthesis of nanostructured materials and functional devices: Processing, modelling, and diagnostics, *Prog. Energy Combust. Sci.*, 55, 1-59.
- Liberini, M., De Falco, G., Scherillo, F., Astarita, A., Commodo, M., Minutolo, P., D'Anna, A., Squillace A. 2016, Nano-TiO<sub>2</sub> coatings on aluminum surfaces by aerosol flame synthesis, *Thin Solid Films*, 609, 53-61.
- Mahdi, R.I., Gan, W.C., Abd Majid, W.H. 2014, Hot plate annealing at a low temperature of a thin ferroelectric P(VDF-TrFE) film with an improved crystalline structure for sensors and actuators, *Sensors (Basel)*, 14, 19115-19127.
- Martin, N., Rousselot, C., Rondot, D., Palmino, F., Mercier, R. 1997, Microstructure modification of amorphous titanium oxide thin films during annealing treatment, *Thin Solid Films*, 300, 113-121.
- McCracken C., Dutta P.K., Waldman W.J. 2016, Critical assessment of toxicological effects of ingested nanoparticles, *Environmental Science: Nano*, 3, 256–282.
- McCormick, J.R., Zhao, B., Rykov, S.A., Wang, H., Chen, J.G. 2004, Thermal Stability of Flame-Synthesized Anatase TiO<sub>2</sub> Nanoparticles, *Journal of Physical Chemistry B*, 108, 17398-17402.
- Starke, E.A., Staley, J.T., 1996, Application of modern aluminum alloys to aircraft, *Progress in Aerospace Sciences* 32, 131-172.
- Williams, J.C., Starke, E.A, 2003, Progress in structural materials for aerospace systems, *Acta Materialia* 51, 5775-5799.